International Journal of Electronics
Publication details, including instructions for authors and subscription information:
http://www.tandfonline.com/loi/tetn20

Faster techniques to evolve wavelet coefficients for better fingerprint image compression

K.T. Shanavaz [a] & P. Mythili [a]

[a] Division of Electronics, School of Engineering, Cochin University of Science & Technology , Kochi , Kerala , India

Published online: 13 Sep 2012.

International Journal of Electronics, 2013
Vol. 100, No. 5, 655–668, http://dx.doi.org/10.1080/00207217.2012.720944

Faster techniques to evolve wavelet coefficients for better fingerprint image compression

K.T. Shanavaz* and P. Mythili

Division of Electronics, School of Engineering, Cochin University of Science & Technology, Kochi, Kerala, India

(*Received 7 September 2011; final version received 15 July 2012*)

In this article, techniques have been presented for faster evolution of wavelet lifting coefficients for fingerprint image compression (FIC). In addition to increasing the computational speed by 81.35%, the coefficients performed much better than the reported coefficients in literature. Generally, full-size images are used for evolving wavelet coefficients, which is time consuming. To overcome this, in this work, wavelets were evolved with resized, cropped, resized-average and cropped-average images. On comparing the peak- signal-to-noise-ratios (PSNR) offered by the evolved wavelets, it was found that the cropped images excelled the resized images and is in par with the results reported till date. Wavelet lifting coefficients evolved from an average of four 256×256 centre-cropped images took less than 1/5th the evolution time reported in literature. It produced an improvement of 1.009 dB in average PSNR. Improvement in average PSNR was observed for other compression ratios (CR) and degraded images as well. The proposed technique gave better PSNR for various bit rates, with set partitioning in hierarchical trees (SPIHT) coder. These coefficients performed well with other fingerprint databases as well.

Keywords: wavelets; lifting scheme; evolved transforms; genetic algorithm (GA); image compression; fingerprint

1. Introduction

The aim of image compression is to gain the best possible image quality at an allotted storage facility. It is needed for easy archiving and faster transmission over band-limited communication channels. It finds a significant role in some vital areas like forensic, medical applications, law enforcement and border security. A mathematical morphology pre-processing algorithm to improve the overall image quality in image compression systems and data protection techniques were proposed by Vizireanu and Preda (2005), Vizireanu (2007, 2008), Udrea and Vizireanu (2007, 2009) and Preda and Vizireanu (2007, 2010, 2011a,b).

To overcome the long delay involved in transmitting fingerprint images over band-limited communication channels, the Federal Bureau of Investigation (FBI) fingerprint identification division has adopted wavelet scalar quantisation (WSQ) as standard for

*Corresponding author. Email: shanavazkt@cusat.ac.in

fingerprint image compression (FIC) (Maltoni, Maio, Jain, and Prabhakar 2009). Wavelet-based image compression (Daubechies 1992; Lewis and Knowles 1992; Suresh, Sudha, and Sukanesh 2009) is very promising, since it examines the image signal at different resolutions. Discrete wavelet transform (DWT) (Daubechies 1992) decomposes the original image to horizontal, vertical and diagonal components. Biorthogonal wavelet (Taubman and Marcellin 2002) has both symmetry and compact support. Many wavelets and techniques have been reported in literature till date (Mallat 1989; Daubechies 1992; Shapiro 1993; Sweldens 1996; Said and Pearlman 1996; Mallat 1999). The hand-designed classical cdf9/7 biorthogonal wavelet introduced in 1992 by Cohen, Daubechies, and Feauveau (cdf) (Cohen, Daubechies, and Feauveau 1992) is used by the FBI fingerprint compression standard (Bradley, Brislawn and Hopper 1993; Babb 2007). The hand-designed cdf9/7 DWT was represented by four sets of coefficients (Babb 2007). Peak-signal-to-noise-ratio (PSNR) and root-mean-squared-error (RMSE) were the two measures of image compression performance (Shanavaz and Mythili 2010). The lifting scheme (Sweldens 1996, 1997; Daubechies and Sweldens 1998) is an efficient way to represent hand-designed wavelets with fewer coefficients. This was done by factorising the polyphase matrix of the wavelet into elementary matrices (Daubechies and Sweldens 1998). Many factorisations of cdf9/7 wavelet exist.

Several researchers have evolved wavelet coefficients using GA (Goldberg 1989; Sivanandan and Deepa 2008; Giri, Rao, and Chattopadhyay 2009). Babb (2007) evolved a total of 128 classical cdf9/7 coefficients, employing four levels MRA. The GA used a population of 240–280 chromosomes with more than 15,000 generations and the huge amount of computational complexity demanded supercomputers for evolving the coefficients. With 80 fingerprint images in the database, the evolved transform improved the average PSNR by 0.76 dB. Grasemann and Mikkulainen (2005) used the co-evolutionary algorithm and properties of lifting by which specialised wavelets were evolved for FIC. Initial coefficients for GA evolution were taken randomly from a Gaussian distribution. Each individual had been evaluated 10 times on average. For a population size of 150 for each of the seven parallel sub-populations, it performed 1500 evaluations in each of the 500 generations in a run. The approach was highly time-consuming. The algorithm took 60 h on a 3 GHz Xeon Processor. An average PSNR improvement of 0.75 dB was reported. Shanavaz and Mythili (2010) described a method in which cdf9/7 lifting coefficients were evolved using GA. A population size of 250 and 1000 generations were used. The algorithm took 33 h on an AMD Athlon 2.39 GHz Processor with 750 MB memory. Over 35.9119 dB average PSNR offered by the hand-designed classical cdf9/7 wavelet, an improvement of 0.9306 dB was reported. Considering the speed of evolution of the lifting coefficients and also to have a fair comparison with the results in the previous work, the symmetric lifting scheme (Taubman and Marcellin 2002; Shanavaz and Mythili 2010) with only four coefficients has been used here.

In this work, cdf9/7 lifting coefficients were evolved with different image sets like resized, cropped, resized-average and cropped-average fingerprint images. This has overcome the computational complexity and time consumption of the evolution process. The results obtained have been compared with the results available in literature. The rest of the article is structured as follows. Section 2 describes the methodology of the proposed work of evolving lifting coefficients and the development of training image sets (TIS) for FIC using GA. Results and discussions are provided in Section 3 and Section 4 concludes the article.

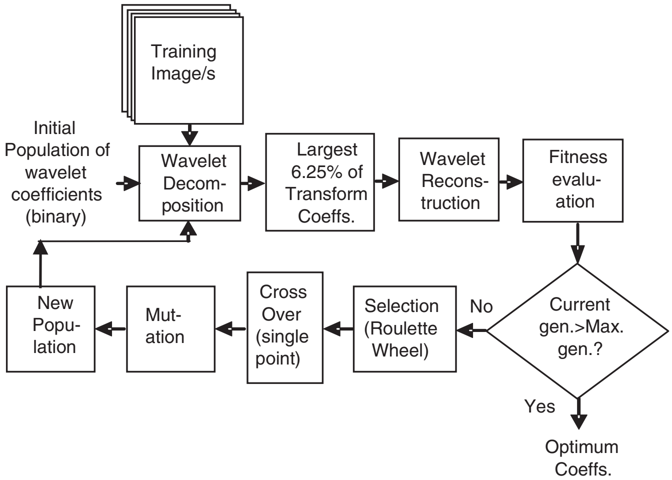

Figure 1. Block diagram of the evolutionary algorithm (GA) for optimising cdf9/7 lifting coefficients for FIC.

2. Methodology

2.1. *Evolution of lifting filter coefficients*

In the present work, GA has been used to evolve symmetrical lifting coefficients of cdf9/7 (Taubman and Marcellin 2002; Shanavaz and Mythili 2010). Compared to the hand-designed cdf9/7 wavelet system, which consist of 16 coefficients, the symmetrical lifting system consists of only 4 coefficients. Use of a lesser number of lifting coefficients enables faster evolution of coefficients. The evolved lifting coefficients, in turn, take lesser time to compress the fingerprint images. The block diagram of the evolutionary GA algorithm for evolving optimal cdf9/7 lifting coefficients for FIC is shown in Figure 1. As in the work of Shanavaz and Mythili (2010), binary GA has been used for the evolution.

Wavelet decomposition block transforms the training images to the wavelet domain using the initial population of chromosomes comprising lifting coefficient sets. To fix the CR to 16:1 the largest 6.25% of image transform coefficients are kept for image reconstruction and the remaining coefficients are set to zero. The quality of the reconstructed image/s is calculated in terms of PSNR. This PSNR serves as the fitness function of the GA. The associated chromosomes are ranked according to their fitness. Then, only the best are selected to continue for reproduction. Cross-over and mutation operations are performed on the selected chromosomes to produce a new set of chromosomes. The above operations are repeated with the new population until an optimum set of coefficients is evolved. The best set of evolved coefficients corresponds to the best PSNR for the TIS. These coefficients are used to find the average improvement in PSNR over 80 fingerprint images in the database.

2.2. *Parameters*

Each set of four coefficients are represented by a 68 bit binary chromosome. Each coefficient has a length of 17 bits, out of which the first bit represents sign and the other 16 bits represent the coefficient value. Randomly mutated copies of the symmetrical lifting coefficients of cdf9/7 are used to create the initial GA population. In order to have a fair comparison with the previous work, the parameters used by Shanavaz and Mythili (2010) are used in this work. The population size for GA evolution is fixed as 250 and the number of generations is 1000. The algorithm used Roulette wheel selection and single point crossover. Crossover rate $P_c = 0.7$, mutation rate $P_m = 0.0075$ and elitism = 1. The developed algorithm was implemented in Matlab.

2.3. *Development of an optimum TIS*

The TIS is derived from the image set B of the DB1 database in the fingerprint verification competition (FVC) 2000 database. The image set B contains 80 fingerprint images. Each image has a size 300×300 pixels and a resolution of 500 dpi. A typical fingerprint image is shown in Figure 2. In the previous works (Grasemann and Mikkulainen 2005; Babb 2007; Shanavaz, and Mythili 2010) the TIS comprised four numbers of full-size (300×300 pixels) representative fingerprint images. In the present work, to start with, a TIS with only one image of full size (300×300 pixels) was used for evolution. Images were added in the image data set one by one up to 10. Average improvement in PSNR over hand-designed wavelet (Villasenor, Belzer, and Lia 1995; Davis and Nosratinia 1998) for various nos. of training images were observed and plotted in Figure 3. A maximum improvement of 1.012 dB in average PSNR above the hand-designed cdf9/7 wavelet over the 80 fingerprint images was obtained. The training set comprised five full-size fingerprint images (TIS_300). The algorithm was able to evolve the coefficients in 11.29 h on an Intel Xeon

Figure 2. A typical fingerprint image (300×300 pixels).

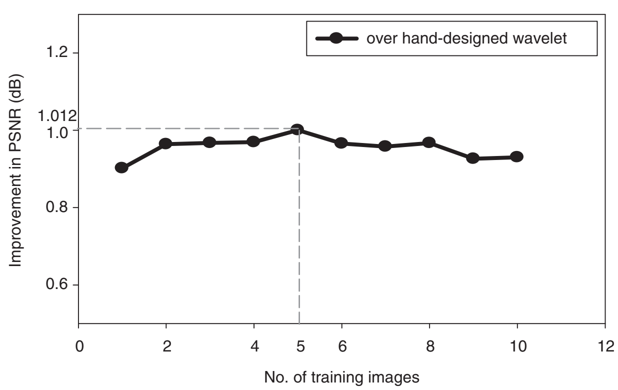

Figure 3. Improvement in PSNR over classical wavelet for various numbers of training images.

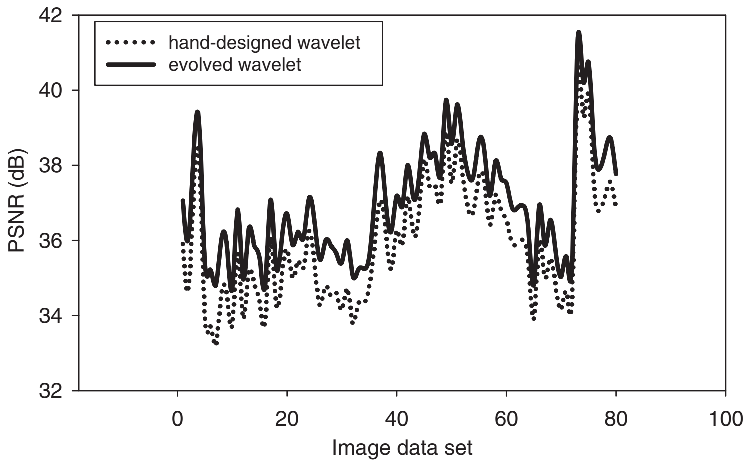

Figure 4. PSNR for hand-designed wavelet and wavelet coefficients evolved from five full-size (300 × 300 pixels) fingerprint images for CR = 16 : 1.

3.00 GHz processor with 6 GB memory. With one image in the TIS, the evolution took 2.26 h. With 10 images, the time taken was 23.03 h. For 2 to 4 and 6 to 8 nos. of training images, the improvement in PSNR was slightly less. For 1, 9 and 10 nos. of training images, the improvement in PSNR was even less. A plot of PSNR for classical wavelet and coefficients evolved from TIS_300 for CR 16:1 is shown in Figure 4. For all the 80 images, the performance of the evolved wavelet was much better than that of the hand-designed wavelet. It shows a maximum PSNR improvement of 1.599 dB for the image 101_7.tif and minimum of 0.681 dB for the image 106_5.tif.

To further study the effects of the training image sets on the speed and quality of coefficients, the fingerprint images were modified to build different training sets. Coefficients were evolved using each set and the corresponding PSNR and computational speed were observed. In this work, four training sets comprising various numbers of fingerprint images with different sizes, resolution etc. were derived as described below.

2.3.1. *Training Image Set 1 (TIS1)*

As mentioned earlier, the maximum average PSNR was obtained with the training set comprising five full-size fingerprint images (TIS_300). So, this image data set consists of five images with their size reduced by cropping at the centre. The cropped training image sets TIS1_256, TIS1_128, TIS1_64, TIS1_32 of sizes 256 × 256, 128 × 128, 64 × 64, 32 × 32 pixels respectiveley were used for evolution. Figure 5 represents a cropped image of size 128 × 128 pixels (TIS1_128).

2.3.2. *Training Image Set 2 (TIS2)*

Similar to TIS1, five images are present in this image set as well. Here, the image data sets TIS2_256, TIS2_128, TIS2_64, and TIS2_32 were derived by resizing the five individual images to 256 × 256, 128 × 128, 64 × 64, 32 × 32 pixels sizes respectively. Figure 6 depicts a

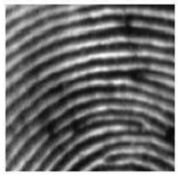

Figure 5. A cropped fingerprint image of size 128 × 128 pixels (TIS1_128).

Figure 6. A resized fingerprint image of size 128 × 128 pixels (TIS2_128).

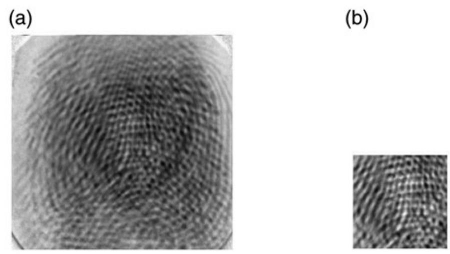

Figure 7. Average of four fingerprint images: (a) full-size (300 × 300 pixels), (b) cropped to 128 × 128 pixels (TIS3_128).

resized image of size 128 × 128 pixels (TIS2_128). In this way the whole fingerprint image is considered.

2.3.3. *Training Image Set 3 (TIS3)*

This set contains only one image which is obtained by averaging the component images. To begin with, average of two images was used for GA evolution. Subsequently, images were appended in the data set one by one up to 10. The maximum PSNR was obtained from the average of four images. So, TIS3_256, TIS3_128, TIS3_64, TIS3_32 were derived by averaging four component images cropped to 256 × 256, 128 × 128, 64 × 64, 32 × 32 pixel sizes respectively. TIS3 with the average of four full-size images and the average of four images cropped to a size of 128 × 128 pixels (TIS3_128) are shown in Figure 7.

2.3.4. *Training Image Set 4 (TIS4)*

Similar to TIS3, only one image is present in this image set too. Training image sets, TIS4_256, TIS4_128, TIS4_64, and TIS4_32 were obtained from the average of four

Figure 8. Average of four resized fingerprint images of size 128 × 128 pixels (TIS4_128).

individual images resized to 256 × 256, 128 × 128, 64 × 4, 32 × 32 pixel sizes respectively. Figure 8 represents the average of four resized images of size 128 × 128 pixels (TIS4_128).

It was observed that the evolved coefficients yielded reduced PSNR compared to the theoretical lifting coefficients when resized/cropped images with sizes below 32 × 32 were used.

The training image sets TIS1 to TIS4 were applied to the evolutionary algorithm in Figure 1. The algorithm was run several times. The optimum lifting coefficients evolved were employed to find the average improvement in PSNR for CR 16:1 over 80 fingerprint images. These coefficients were used to compute the improvement in PSNR for other CRs too. Besides this, the performances of the coefficients on degraded images were also studied. To perform this, the quality of the input image was degraded to various amounts by setting certain percentages of lower pixel values to zero. The percentage degradation was calculated as (Shanavaz and Mythili 2010)

$$\text{Degradation} = \frac{\text{No. of pixels set to zero}}{\text{Total no. of pixels}} \times 100\%. \tag{1}$$

The evolved coefficients were used with SPIHT (set partitioning in hierarchical trees) (Said and Pearlman 1996; SPIHT 2004) algorithm without arithmetic coder to observe their performance. In addition to the above, the performance of these coefficients was tested on other fingerprint databases too.

3. Results and discussion

3.1. *Improvement in PSNR for various training image sets*

The different data sets TIS1, TIS2, TIS3 and TIS4 with suitable number of images to give the maximum PSNR were constructed as mentioned in the previous section. They were used to evolve optimum coefficients giving maximum PSNR for CR 16:1. These coefficients were employed to find the average improvement in PSNR over 80 fingerprint images. The results are compared with the result of the image set TIS_300, which contains full-size images for validation purposes. Figure 9 shows the average improvement in PSNR for each image size in all the above image data sets. As illustrated in the figure, the performance of TIS1 and TIS3 with cropped images is better than the TIS2 and TIS4 with resized images. It can also be seen that TIS3_256 with cropped average images perform better compared to other image sets except TIS_300. The average PSNR improvement of 1.012 dB corresponding to TIS_300 is shown as a single point in Figure 9. PSNR improvement of 1.009 dB was achieved from TIS3_256. The evolution took only 1.692 h. So, at the expense of just 0.003 dB (a negligibly small value), 81.35% improvement in the speed of evolution could be achieved. The evolution-time and PSNR are better than the

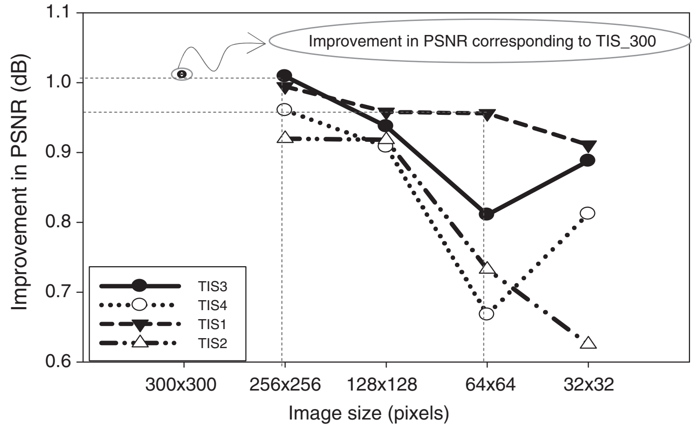

Figure 9. Comparison of the average PSNR improvement for TIS1, TIS2, TIS3 and TIS4.

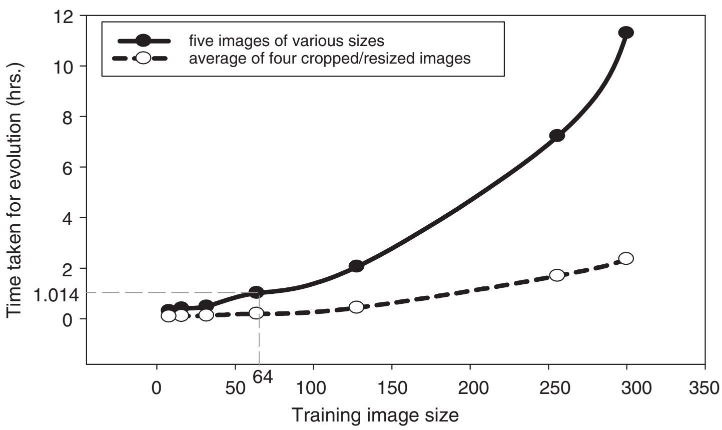

Figure 10. Plot of average evolution-time versus training image size.

previous results (Grasemann and Mikkulainen 2005; Babb and Moore 2007; Babb, Moore, and Peterson 2009; Salvador, Moreno, Riesgo, and Sekanina 2010). The plot of average evolution-time taken with image sets TIS1 to TIS4 is shown in Figure 10. It is obvious that the images with reduced size caused faster evolution with little compromise in PSNR improvement. For example, TIS1_64 took just 1.014 h yielding 0.956 dB improvement in PSNR. Compared to TIS_300 improvement in PSNR differed by just 0.056 dB, which is too small. But, the speed of evolution was increased by 91.02%. Compared to the TIS in the published work (Shanavaz and Mythili 2010), TIS1_64 gave 88.81% increase in speed of evolution and 0.025 dB improvement in PSNR. In the case of averaged images, TIS3_32 and TIS4_32 surpassed TIS3_64 and TIS4_64, respectively, with better PSNR and 39.51% increase in speed of evolution. Compared to the existing technique, TIS3_32 offered 98.7% increase in evolution speed only at the expense of 0.043 dB PSNR.

Among all these TISs, the best PSNR improvements of 1.012 dB and 1.009 dB were tendered by TIS_300 and TIS3_256 respectively. So, the rest of this article concentrates on the results related to these TISs. The original image 101_1.tif and the reconstructed images

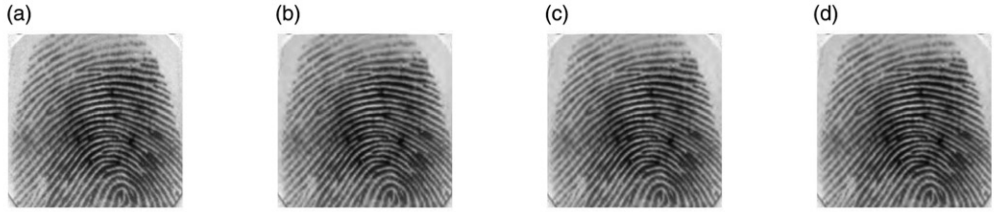

Figure 11. 101_1.tif image (a) original, reconstructed image using (b) classical wavelet (PSNR = 35.908 dB), using evolved coefficients from (c) TIS_300 (PSNR = 37.062 dB) and (d) TIS3_256 (PSNR = 37.069 dB).

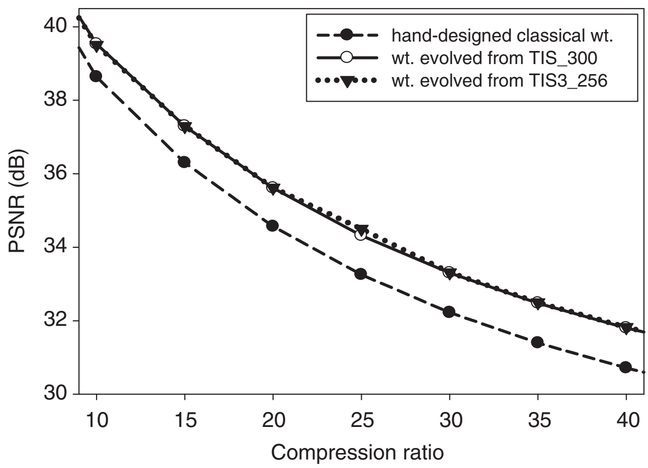

Figure 12. Plot of average PSNRs for classical wavelet and wavelet evolved from TIS_300 and TIS3_256.

corresponding to hand-designed cdf9/7 wavelet, coefficients evolved from TIS1_300 and TIS3_256 are shown in Figure 11.

3.2. *Improvement in PSNR for various CRs*

The evolved coefficients exhibit PSNR improvement for other CRs as well. Figure 12 compares the PSNRs of the evolved and hand-designed wavelets for various CRs. For all values of CRs the evolved wavelets yielded better PSNR over the classical wavelet. The wavelets evolved from the above two different TISs (TIS_300 & TIS3_256) provided almost identical PSNRs.

3.3. *PSNRs of degraded images*

Figure 13 illustrates the comparison of average PSNRs of degraded images for CR = 10:1, computed from hand-designed wavelet and wavelet evolved from TIS3_256. Here, the quality of the input images were degraded to various amounts by setting certain percentages of lower pixel values to zero. Percentage degradation was calculated using Equation (1) (Shanavaz and Mythili 2010).

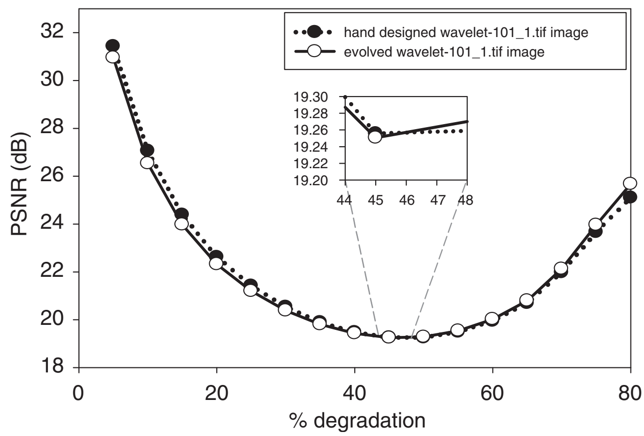

Figure 13. Comparison of average PSNRs of degraded images for CR = 10 : 1, computed from hand-designed wavelet and wavelet evolved from TIS3_256.

Figure 14. 101_1.tif image (a) 15% degraded, reconstructed with (b) classical wavelet (PSNR = 22.982 dB) (c) evolved wavelet from TIS_300 (PSNR = 23.088 dB) (d) from TIS3_256 (PSNR = 23.056 dB).

As shown in Figure 13, the PSNR corresponding to the classical wavelet was better than the evolved PSNR for lower values of degradation. The evolved PSNR became better beyond 46% of degradation. For lower CRs, evolved coefficients started to surpass the classical coefficients at higher degradation values. For example, with CR = 5, the evolved PSNR crossed the classical PSNR at 80% degradation. For CRs above 20:1 evolved coefficients outperformed the classical wavelets for all degradation values. The results were similar in the case of coefficients evolved from TIS_300. Figure 14 shows the 101_1.tif image with 15% degradation (i.e., 15% of lower pixel values were set to zero). The images reconstructed using classical as well as evolved coefficients for CR 20:1 are also shown. The PSNR of the degraded image owing to evolved wavelets was slightly better.

3.4. *PSNR improvement with SPIHT coding*

There was reasonable improvement in PSNR when evolved coefficients were used with SPIHT (Said and Pearlman 1996; SPIHT 2004) algorithm without arithmetic coder. Figure 15 compares the average PSNR with SPIHT coder for various bits/pixel (bit-rate)

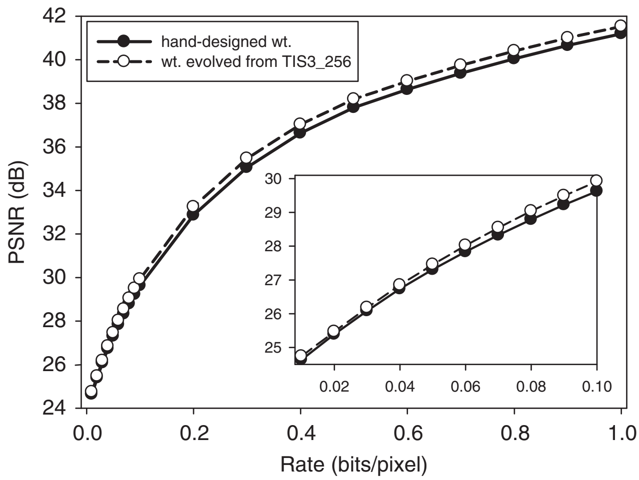

Figure 15. Comparison of average PSNRs between classical and wavelet evolved from TIS3_256 used in the SIPHT algorithm for various bit-rates.

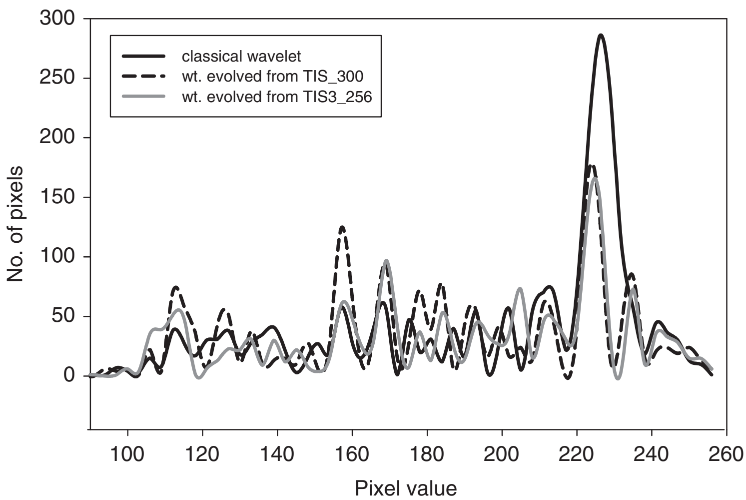

Figure 16. Absolute difference between histogram values of 101_1.tif image and the images reconstructed with classical wavelet and wavelet evolved from TIS_300 and TIS3_256.

values for classical and evolved wavelets. It can be seen that the wavelet evolved from TIS3_256 outperformed the classical wavelet for all bit-rates. The wavelet evolved from TIS_300 also confirmed the results.

3.5. *Comparison of histogram differences*

Direct visual inspection of the images would not probably give sufficient information for a fair judgement. Figure 16 compares the efficiency of the evolved wavelets in FIC. Here the absolute difference between histogram values of 101_1.tif image and the images reconstructed with hand-designed wavelet, wavelet evolved from TIS_300 and TIS3_256 are plotted. As illustrated in the figure, histogram differences of the images reconstructed from evolved wavelets are much less than that of the image reconstructed from hand-designed wavelet. It can also be seen that the minimum absolute histogram difference is offered by the wavelet evolved from TIS3_256, and hence it performs better than that evolved from TIS_300.

3.6. *Improvement in PSNR for other fingerprint databases*

The performance of the evolved coefficients on the other databases of FVC was studied. Except in a few cases, the evolved coefficients offered better PSNR.

4. Conclusion

This article presents faster techniques for evolving wavelet coefficients, optimised for better compression and reconstruction of fingerprint images. Here, a lifting scheme combined with GA is used to evolve better lifting coefficients of the cdf9/7 wavelet. The hand-designed cdf9/7 wavelet can be represented by a few numbers of lifting coefficients. So, they are evolved at a faster rate using GA. Usually, full-size images are used for evolving wavelets. This evolution process is too slow. To speed up this, in this article, wavelets were evolved with different image sets like resized, cropped, resized-average and cropped-average images. Comparing the PSNRs offered by the evolved wavelets, it was found that the cropped images outperformed the resized images and is in par with the results reported so far. It was observed that, the wavelet evolved from cropped images outperformed the wavelet evolved from resized images. The wavelet evolved from an average of four 256×256 centre-cropped images took less than 1/5th the evolution time reported in literature. Besides increasing the computational speed by 81.35%, the evolved coefficients offered 1.009 dB improvements in average PSNR over 80 fingerprint images in the database. At the cost of a very small amount of PSNR, additional reduction in evolution-time could be achieved. The evolved coefficients exhibit improvement in PSNR for other CRs too. For higher CRs, the evolved coefficients outperformed the classical wavelets in compressing degraded images. There was reasonable improvement in PSNR when evolved coefficients were used with SPIHT algorithm. Except in a few cases, the coefficients evolved for the database DB1_B of FVC 2000 offered better PSNR when applied to the other fingerprint databases of different sizes and clarity. Image compression can be further improved by using application-specific optimised wavelets for medical, satellite and digital photography applications. One of the factors that improves the performance of the evolved wavelet is a properly designed training data set. Therefore, techniques can be developed to design an optimum training data set, which improves compression performance.

References

Babb, B. (2007), 'Evolved Transforms Surpass the FBI Wavelet for Improved Fingerprint Compression and Reconstruction', in *Proceedings of the 2007 Conference Companion on Genetic and Evolutionary Computation*, London, July 7–11, pp. 2603–2606.

Babb, B., and Moore, F. (2007), 'The Best Fingerprint Compression Standard Yet', in *Systems, Man and Cybernetics, IEEE International Conference*, pp. 2911–2916.

Babb, B., Moore, F., and Peterson, M. (2009), 'Improved Multiresolution Analysis Transforms for Satellite Image Compression and Reconstruction Using Evolution Strategies', in *Proceedings of the 11th Annual Conference Companion on Genetic and Evolutionary Computation* , ACM, 2009, pp. 2547–2552.

Bradley, J., Brislawn, C., and Hopper, T. (1993), 'The FBI Wavelet/Scalar Quantization Standard for Gray-scale Fingerprint image Compression', in *SPIE Proceedings Visual Information Processing II,* 1961, pp. 293–304.

Cohen, A., Daubechies, I., and Feauveau, J.-C. (1992), 'Biorthogonal Bases of Compactly Supported Wavelets', *Communications on Pure and Appied. Mathematics*, 45, 485–560.

Daubechies, I. (1992), *Ten Lectures on Wavelets*, Philadelphia, Pennsylvania: SIAM.

Daubechies, I., and Sweldens, W. (1998), 'Factoring Wavelet Transforms into Lifting Steps', *Journal of Fourier Analysis and Applications*, 4, 245–267.

Davis, G., and Nosratinia, A. (1998), 'Wavelet-based Image Coding: An Overview,' in *Appl. and Comp. Control, Signals and Circuits*, ed. Biswa Nath Datta, Boston, NY, USA: Springer-Verlag.

Giri, Chandan; Rao, Mallikarjuna B., and Chattopadhyay, Santanu (2009), 'Split Variable-length Input Huffman Code with Application to Test Data Compression for Embedded Cores in SOCs', *International Journal of Electronics*, 96, 935–942.

Goldberg, D. (1989), *Genetic Algorithms in Search, Optimization, and Machine Learning* (1st ed.), Boston, MA, USA: Addison-Wesley.

Grasemann, U., and Mikkulainen, R. (2005), 'Effective Image Compression Using Evolved Wavelets', in *Proceedings of the 7th Annual Genetic and Evolutionary Computation Conference,* Washington DC, USA, June 25–29, pp. 1961–1968.

Lewis, A.S., and Knowles, G. (1992), 'Image Compression Using the 2D Wavelet Transform', *IEEE Transactions on Image Processing*, 1, 244–250.

Mallat, S. (1989), 'A Theory for Multiresolution Signal Decomposition: The Wavelet Representation', *IEEE Transactions on Pattern Analysis and Machine Intelligence*, 11, 674–693.

Mallat, S. (1999), *A Wavelet Tour of Signal Processing*, San Diego, California, USA: Academic Press, Elsevier.

Maltoni, D., Maio, D., Jain, A.K., and Prabhakar, S. (2009), *Handbook of Fingerprint Recognition* (2nd ed.), London, UK: Springer-Verlag.

Preda, R.O. and Vizireanu, D.N. (2007), 'Blind Watermarking Capacity Analysis of MPEG2 Coded Video', *IEEE TELSIKS 8th International Conference on Telecommunication in Modern Satellite, Cable and Broadcasting Services*, pp. 465–468.

Preda, R.O., and Vizireanu, D.N. (2010), 'A Robust Digital Watermarking Scheme for Video Copyright Protection in the Wavelet Domain', *Measurement*, 43, 1720–1726.

Preda, R.O., and Vizireanu, D.N. (2011a), 'A Robust Wavelet Based Video Watermarking Scheme for Copyright Protection Using the Human Visual System', *Journal of Electronic Imaging*, 20, 013 022.

Preda, R.O., and Vizireanu, D.N. (2011b), 'Quantization Based Video Watermarking in the Wavelet Domain with Spatial and Temporal Redundancy', *International Journal of Electronics*, 98, 393–405.

Said, A., and Pearlman, W.A. (1996), 'A New, Fast and Efficient Image Codec based on Set Partitioning in Hierarchical Trees', *IEEE Transactions on Circuits and Systems for Video Technology*, 6, 243–250.

Salvador, R., Moreno, F., Riesgo, T., and Sekanina, L. (2010), 'Evolutionary Design and Optimization of Wavelet Transforms for Image Compression in Embedded Systems', in *Proceedings of the NASA/ESA Conference on Adaptive Hardware and Systems*, pp. 171–178.

Shanavaz, K.T., and Mythili, P.(2010), 'An Improved Technique for Evolving Wavelet Coefficients for Fingerprint Image Compression', in *Proceedings of IEEE International Conference on Communication Control and Computing Technologies,* Ramanathapuram, India, October, pp. 665–669.

Shapiro, J.M. (1993), 'Embedded Image Coding Using Zerotrees of Wavelet Coefficients', *IEEE Transactions on Signal Processing*, 41, 3445–3462.

Sivanandan, S.N., and Deepa, S.N. (2008), *Introduction to Genetic Algorithms*, Berlin/Heidelberg: Springer-Verlag.

SPIHT (2004), 'SPIHT Algorithm in MATLAB Program Language' http://www.cipr.rpi.edu/research/SPIHT/spiht3.html.

Suresh, G.R., Sudha, S., and Sukanesh, R. (2009), 'Shape Adaptive Wavelet Transform for Magnetic Resonance Images Coding', *International Journal of Electronics*, 96, 613–622.

Sweldens, W. (1996), 'The Lifting Scheme: A Custom-design Construction of Biorthogonal Wavelets', *Journal of Applied and Computational Harmonic Analysis*, 3, 186–200.

Sweldens, W. (1997), 'The Lifting Scheme: A Construction of Second-generation Wavelets', *SIAM Journal on Mathematical Analysis*, 29, 511–546.

Taubman, D., and Marcellin, M. (2002), *JPEG2000: Image Compression Fundamentals, Standards, and Practice*, Boston/Dordrecht/London: Kluwer Academic Publishers.

Udrea, R.M., and Vizireanu, D.N. (2007), 'Iterative Generalization of Morphological Skeleton', *Journal of Electronic Imaging*, 16, 010501-1–010501-3.

Udrea, R.M., and Vizireanu, D.N. (2009), 'Visual-oriented Morphological Foreground Content Grayscale Frames Interpolation Method', *Journal of Electronic Imaging*, 18, 020502-1–020502-3.

Villasenor, J., Belzer, B., and Lia, J. (1995), 'Wavelet Filter Evaluation for Image Compression', *IEEE Transactions on Image Processing*, 2, 1053–1060.

Vizireanu, D.N. (2007), 'Generalizations of Binary Morphological Shape Decomposition', *Journal of Electronic Imaging*, 16, 01302-1–01302-6.

Vizireanu, D.N. (2008), 'Morphological Shape Decomposition Interframe Interpolation Method', *Journal of Electronic Imaging*, 17, 013007-1–013007-5.

Vizireanu, D.N. and Preda, R.O. (2005), 'A New Digital Watermarking Scheme for Image Copyright Protection Using Wavelet Packets', *IEEE TELSIKS 7th International. Conference on Telecommunication inModern Satellite, Cable and Broadcasting Services*, 2005, 518–521.